Journal of Thermal Analysis and Calorimetry, Vol. 85 (2006) 3, 699–706

ISOTROPIC TRANSITION BEHAVIOUR OF AN AMPHIPHILIC DI-BLOCK COPOLYMER UNDER PRESSURE
Carbon dioxide or mercury as pressure medium

S. A. E. Boyer[1, 2, 5], *J-P. E. Grolier*[2], *L. Pison*[2], *C. Iwamoto*[1], *H. Yoshida*[3*, 5] *and T. Iyoda*[4, 5]

[1]Department of Applied Chemistry, Graduate School of Engineering, Tokyo Metropolitan University (TMU), Hachiouji-Shi, Tokyo, Japan
[2]Laboratory of Thermodynamics of Solutions and Polymers (LTSP), Blaise Pascal University, Clermont-Ferrand, France
[3]Department of Applied Chemistry, Faculty of Urban Environmental Sciences, Tokyo Metropolitan University (TMU), Hachiouji-Shi, Tokyo, Japan
[4]Chemical Resources Laboratory, Tokyo Institute of Technology (TIT), Midori-Ku, Yokohama, Japan
[5]CREST-Japan Science and Technology Agency

The present work deals with the interactions between carbon dioxide, used as pressure medium, either in the gas state (GCO_2) or in the supercritical state ($SCCO_2$) and amphiphilic di-block copolymers PEO_m-*b*-$PMA(Az)_n$. The effect of pressure on the isotropic transition of the PEO*m*-*b*-$PMA(Az)_n$ copolymer was investigated using scanning transitiometry (ST). The experimental results were compared with those measured when using 'relatively inert' mercury (Hg) as pressure medium. Morphological observation of a PEO_m-*b*-$PMA(Az)_n$ thin film submitted to $SCCO_2$ was performed by atomic force microscopy (AFM) to investigate the nano-structure organization. These results indicate the possibility of modifying the nano-structure in a specific way depending on the CO_2 physical state.

Keywords: *amphiphilic di-block copolymers, calorimetric-pVT measurements, interactions, supercritical carbon dioxide*

Introduction

Different fields of application such as petroleum [1, 2], food packaging, pharmaceutical industry, solubility enhancers in supercritical carbon dioxide [3] require the knowledge of interfacial phase behaviour between gaseous molecules and polymers. New application fields appear with the rapid growth of information technology (IT) for which ongoing downscaling of microelectronics evolves into nano-electronics. The development of highly ordered nano-structures in macroscopic area has attracted increasing interest through nano-science and nano-technology breakthroughs in the new generation of microelectronic and optical devices. Since liquid crystals exhibit a rich variety of phases and phase transitions, block copolymer systems are promising candidates for building periodic nano-structures at low-cost by simple self-assembling [4]. Modification of nano-ordered structures formed by block copolymers is a key technology in nano-science. An important feature of self-ordered structures is their reorganization by modification of interface between the two components of block copolymers by a pressurizing fluid, like carbon dioxide CO_2. For this purpose, phase diagrams of the system as functions of thermodynamic independent variables (p, V, T) and volume fraction ϕ of block copolymers must be well established. Similarly, interactions between pressurizing fluids and block copolymers must be characterized.

The first literature report on supercritical phenomena in fluids appeared in 1822 [5, 6]. Although supercritical CO_2 has been preferably used for most supercritical fluid extraction (SFE) studies, other substances also are used as supercritical solvents such as ammonia, argon, freon, propane, xenon and water. Important point in the choice of a supercritical fluid (SF) is the experimental conditions, e.g. temperature and pressure necessary to reach the critical region of the fluid.

Supercritical CO_2 ($SCCO_2$) appears as a good candidate because of relatively low critical temperature and pressure, 304.13 K and 7.375 MPa respectively, coupled with its wide availability and low cost, low toxicity and low reactivity. $SCCO_2$ is known to be used in extraction of nonpolar and slightly polar species such as alkanes, terpenes, aldehydes, esters, and alcohols.

Few studies concern the phase transition behaviour of polymers under 'active' pressurizing hydraulic fluids, in order to analyze precisely the role of interfacial interactions. One study deals with the melting point of various polymers including homo-, and copo-

* Author for correspondence: yoshida-hirohisa@c.metro-u.ac.jp

1388–6150/$20.00

Akadémiai Kiadó, Budapest, Hungary
Springer, Dordrecht, The Netherlands

lymers, namely high density polyethylene (HDPE), low density polyethylene (LDPE), polypropylene (PP), ethylene vinyl acetate copolymers (EVA) under nitrogen (N_2) pressures up to 330 MPa by high pressure DTA [7]. Another shows the effect of CO_2 on the melting behaviour of semicrystalline polymers, namely syndiotactic polystyrene (sPS) and poly(ethylene terephthalate) (PET), using differential scanning calorimetry (Setaram DSC) equipped with high pressure vessel rated to 10 MPa [8].

In this study we investigated the interactions between the active fluid CO_2 and di-block copolymers PEO_m-*b*-$PMA(Az)_n$. Our study was focussed on how the interactions were influenced depending on the physicochemical states of carbon dioxide either as a gas (GCO_2) or a liquid (LCO_2) or as a supercritical fluid ($SCCO_2$). Scanning transitiometry, which combines calorimetric and *pVT* techniques, was used for the thermodynamic investigation. Scanning transitiometry permits to analyse in-situ thermal effects associated to the phase transitions of a polymer submitted simultaneously to barometric and chemical constraints generated by high pressure CO_2. In addition, the supercritical fluid was used to modify the fine nano-scale structure. Experiments were carried over the temperature range from 280 to 420 K and at pressures up to 50 MPa in this work.

Experimental

Materials

Liquid-crystalline amphiphilic di-block copolymers PEO_m-*b*-$PMA(Az)_n$, prepared by atom transfer radical polymerization [9] and used in this study, are composed of hydrophilic poly(ethylene oxide), PEO_m, sequences and hydrophobic 11-[4-(4-butylphenylazo)phenoxy]-undecyl methacrylate, $PMA(Az)_n$, with azobenzene moieties as mesogen connected by flexible spacer, as shown in Scheme 1. In di-block copolymers PEO_m-*b*-$PMA(Az)_n$, *m* and *n* indicate the degrees of polymerization of PEO and PMA(Az) components, respectively. The common differential scanning calorimetry (DSC) study of PEO_m-*b*-$PMA(Az)_n$ gives a clear picture of thermal properties in liquid crystalline polymers. Four phase transitions are ascribed to the melting of PEO, the melting of azobenzene moieties PMA(Az), the smectic (hardly visible) and the isotropic transitions as shown in Fig. 1 [4, 9]. PEO_m-*b*-$PMA(Az)_n$ forms high ordered hexagonal packed PEO cylinders structures by annealing at the isotropic state.

Isotropic transition of di-block copolymers was studied by scanning transitiometry at LTSP-France. PEO_{114}-*b*-$PMA(Az)_{20}$ samples with the respective masses of 0.1967 and 0.3845 g, were investigated under carbon dioxide CO_2 or mercury Hg as pressure media. CO_2 was supplied by SAGA France and used without further purification (purity of 99.5%). The scanning transitiometry experiments with CO_2 were carried out at 5 and 8 MPa. During phase transitions of PEO_m-*b*-$PMA(Az)_n$, CO_2 is either in the gas state or in supercritical state at 5 and 8 MPa, respectively. The nano-structure organization of PEO_{114}-*b*-$PMA(Az)_{46}$ modified by CO_2 was investigated by atomic force microscopy (AFM). Thin films of PEO_{114}-*b*-$PMA(Az)_{46}$ were prepared by Microgravure coating technology (2 mass% toluene solution) and polyethylene terephthalate (PET) was used as a flexible support for the polymer films. The film thickness of PEO_{114}-*b*-$PMA(Az)_{46}$ on PET was about 100 nm. CO_2 for modification was supplied by Taiyo Toyo Sanso Co. Ltd. Japan and used without further purification.

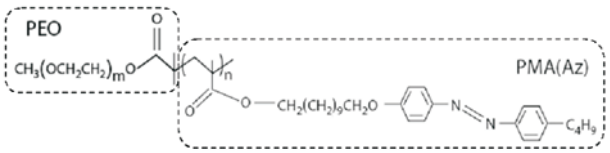

Scheme 1 Amphiphilic di-block copolymers of PEO_m-*b*-$PMA(Az)_n$; *m* and *n* indicating the degrees of polymerization of PEO and PMA(Az) components, respectively

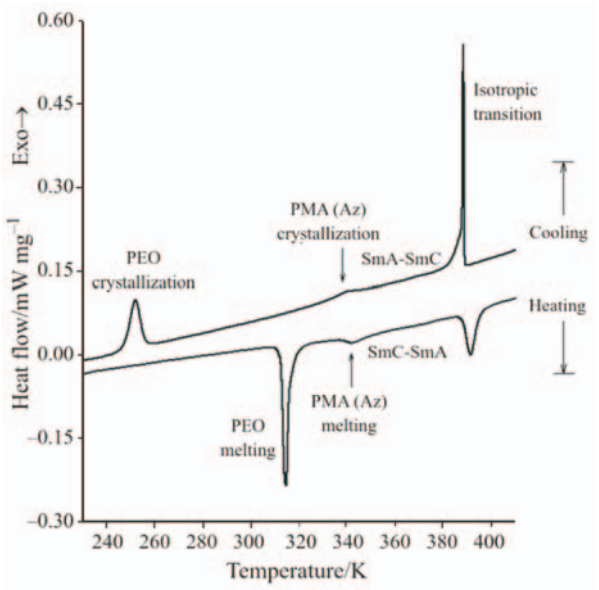

Fig. 1 DSC heating and cooling curves of PEO_{114}-*b*-$PMA(Az)_{20}$ at 2 K min^{-1} under N_2 at 0.1 MPa

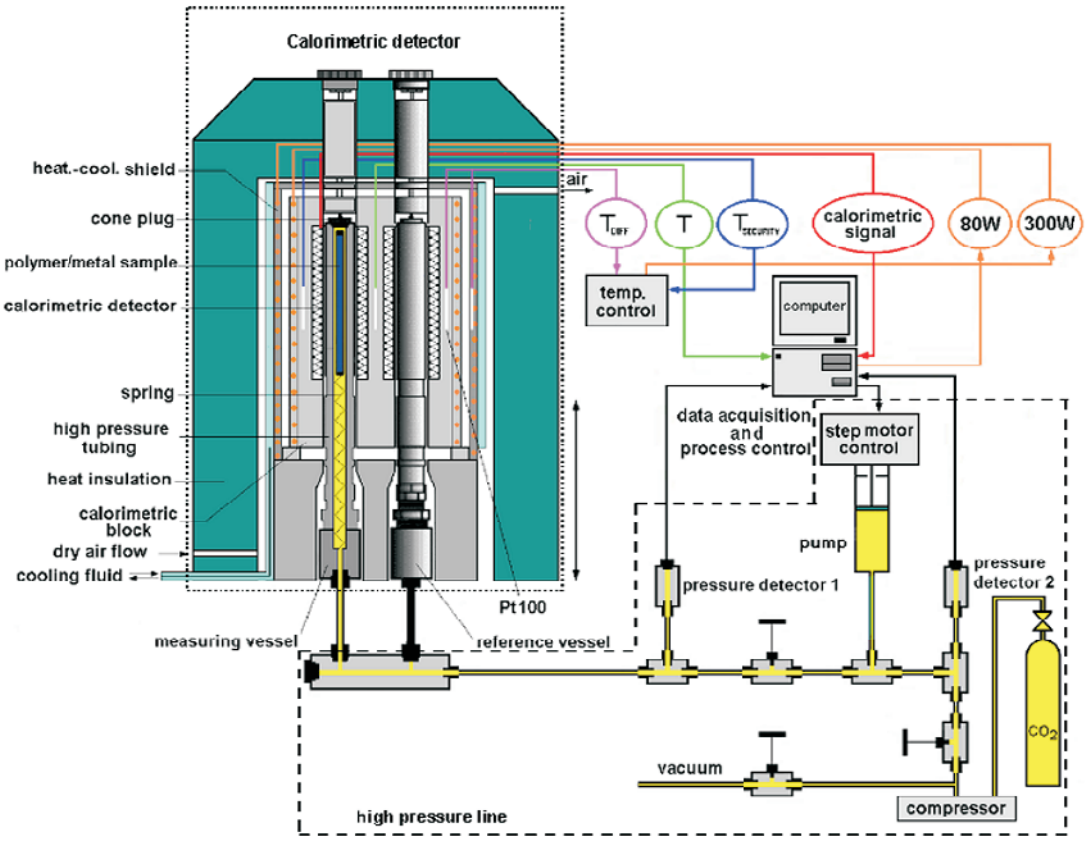

Fig. 2 Schematic view of the transitiometer set-up including the calorimetric detector equipped with high-pressure vessels and a supercritical *pVT* system

Methods

Scanning transitiometry (ST)

The high pressure calorimeter, scanning transitiometer (ST, type BGR TECH model ST-5VI, Warsaw, Poland) is designed to be operated under hydrostatic pressures up to 400 MPa [10, 11]. The whole set-up allows to scan (at a low rate or stepwise) one of the independent thermodynamic variables (*p*, *V* or *T*) while the other independent variable is kept constant. The change of the dependent variable and the concomitant thermal effect related to the system under investigation are recorded simultaneously. In this study, CO_2 was chosen as the pressure transmitting hydraulic fluid. Supercritical scanning transitiometry was described elsewhere by Randzio and Grolier [10] and phase transition modifications of medium density polyethylene (MDPE) were investigated under supercritical methane at pressures up to 100 MPa. The block diagram of the system is schematically illustrated on Fig. 2. An oil pump coupled to a maximator compressor (a booster) is used to generate hydrostatic pressure. Pressure is transmitted to the ST measuring cell via a high pressure line. Pressure is detected by a 400 MPa (Viatran 0-60000 psig) gauge and is displayed directly on a digital manometer with an accuracy of 0.15% (full scale). The resolution of the volumetric system is (5.24±0.04) 10^{-6} cm^3 per motor step. A Labview environment permits to record simultaneously the *p*, *V* and *T* data as well as the associated thermal signals.

The Temperature-Controlled Scanning Calorimetry (TCSC) procedure was selected here with a constant heating rate of 0.2 K min^{-1}. Pressure *p* at 5 and 8 MPa was kept constant by monitoring the volume (*V*) change of the system. As regards the respective role of the measuring and reference vessels, the thermal differential mode was chosen [11]. The reference vessel, not connected to the pressure line, acts as a thermal reference. The measuring vessel contains the polymer sample placed in an open glass ampoule in such a way the polymer is in contact with the hydraulic pressurizing fluid. Calibration of the calorimetric detector was performed with the melting of two standard organic substances: *p*-dibromobenzene and benzoic acid.

Atomic force microscopy (AFM)

The nanostructure of PEO_{114}-*b*-$PMA(Az)_{46}$ di-block copolymer was analyzed using a Shimadzu AFM scanning probe microscope (WET-SPM-9500J3,

Japan) equipped with a tip (Veeco-TAP150) in contact mode. A film sample of the di-block copolymer was set on a polyethylene terephthalate (PET) support [12].

Results and discussion

Polymer samples were submitted to the triple effects: barometric with the CO_2 pressurizing fluid maintained at constant pressure, chemical by using CO_2 as hydrostatic fluid, and thermal by choosing to scan the independent variable *T*. ST measurements under constant hydrostatic CO_2 pressures from 0.1 to 50 MPa were performed over the isotropic transition at slow heating rates, i.e. 0.2 K min^{-1} with CO_2 and 0.1 K min^{-1} with Hg, which are imperative to keep the system closed to the thermodynamic equilibrium. A typical transitiometric curve of the isotropic transition of PEO_{114}-*b*-$PMA(Az)_{20}$ under 5 MPa is represented with the simultaneous thermal (calorimetric signal) and mechanical (volume change shown in steps) effects on Fig. 3. The onset temperature was accepted as the isotropic transition temperature (T_{iso}), transition volume (ΔV_{iso}) and entropy (ΔS_{iso}) were evaluated from mechanical and thermal effects, respectively. In this pressure range with CO_2, no clear change of volume was detected, contrary to what was observed with Hg [13], probably due to the great compressibility of CO_2 and of the CO_2 sorption in the polymer. The CO_2 sorption in the polymer induces a volume change of the polymer. Compensation effects of volume change at phase transition (volume increase) and absorption of gaseous CO_2 in the polymer (volume decrease) indicate a kind of a 'dilution' effect without volume change. With 'inert' Hg as pressure medium, three-phase diagrams (T_{iso}, ΔV_{iso}, ΔS_{iso}) *vs*. *p* corresponding to the thermal and mechanical effects were obtained. With Hg, integration of the change of volume $\Delta V_{iso}/dt$ during temperature scanning was possible to estimate the entropy of the system from the mechanical signal. Using CO_2, insights into the thermophysical properties of the polymer, i.e. two-phase diagrams (T_{iso}, ΔS_{iso}) *vs*. *p*, were obtained from the thermal output.

The transitiometric heating curves under CO_2 pressures of 5 and 8 MPa show an endothermic peak as represented on Fig. 4, and the same pattern was observed with DSC curves under N_2 at 0.1 MPa. Scanning transitiometry permits to investigate in-situ the effect of a pressurizing fluid on the transition, effectively the thermal responses give a clear relation between the isotropic temperature and CO_2 pressures. Different isotropic temperatures were detected after three scans on the same sample at 5 and 8 MPa. The differences observed at these two pressures correspond to the physical state of CO_2. In the gaseous state (GCO_2) at 5 MPa, T_{iso} was shifted to lower temperature by about 3 K, whereas in the supercritical state ($SCCO_2$) at 8 MPa, T_{iso} was practically not changed. This means that the thermodynamic equilibrium is already established during the first run in $SCCO_2$. These results demonstrate the advantage of $SCCO_2$ with which the thermodynamic equilibrium was attained more easily than with GCO_2.

Figure 5 illustrates the quite different shift of T_{iso} *vs*. *p* for PEO_{114}-*b*-$PMA(Az)_{20}$ at the isotropic transition under hydrostatic pressure of 'chemically active' CO_2, compared to what was observed under pressure of 'inert' Hg. The measurements under Hg pressure were obtained in the same way; a detailed description is given elsewhere [14]. The isotropic transition under 'inert' Hg pressure increases with pressure [13]. A linear

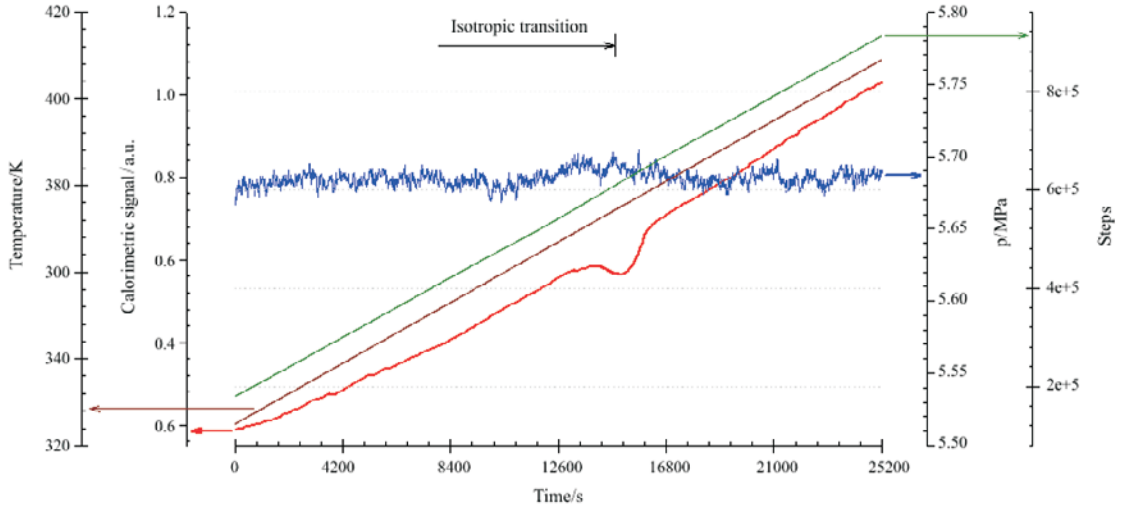

Fig. 3 Isobaric scans over the isotropic transition of {CO_2/PEO_{114}-*b*-$PMA(Az)_{20}$} system under 5 MPa at 0.2 K min^{-1}. At T_{iso}, isotropic transition occurs; the pressure is kept constant through the volume change V_{iso} of the system

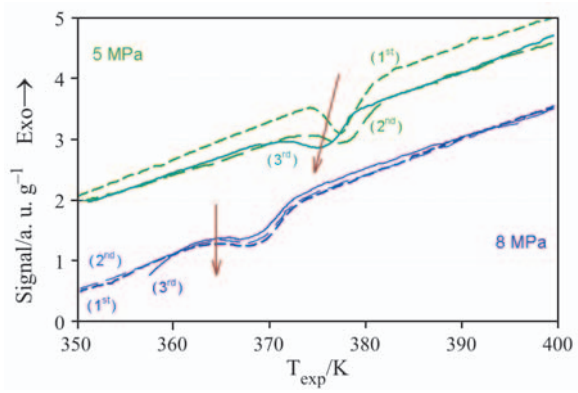

Fig. 4 Transitiometric heating curves for the isotropic transition of {CO_2/PEO_{114}-*b*-PMA(Az)$_{20}$} system under 5 and 8 MPa. Successive heating runs are labelled (1st) (2nd) (3rd)

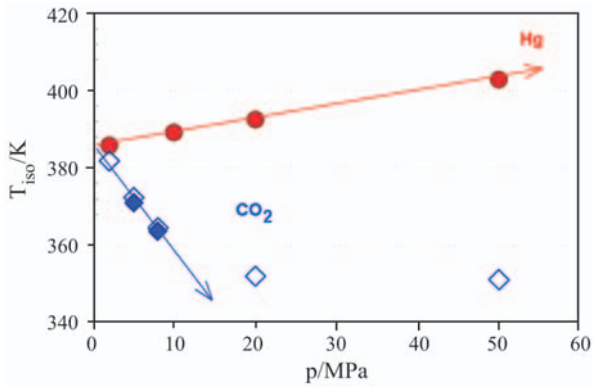

Fig. 5 Isotropic temperature T_{iso} as a function of pressure for {PEO_{114}-*b*-PMA(Az)$_{20}$} system under either Hg (closed circles) or CO_2 (closed diamonds) pressures. T_{iso} trend of {CO_2/PEO_{114}-*b*-PMA(Az)$_{40}$} system, with a mass of copolymer of 0.1052 g, is displayed at high pressure (open diamonds)

shift of the isotropic temperature of {Hg/PEO_{114}-*b*-PMA(Az)$_{20}$} system was calculated directly through the Clapeyron equation. The increase of the isotropic temperature with pressure (dT_{iso}/dp) was found to be 0.35 K MPa^{-1} over the pressure range from atmospheric pressure to 50 MPa. T_{iso} increases with Hg pressure because the pressure limits the degrees of freedom of the molecules that is to say the molecular motions are restricted by hydrostatic pressure. When pressurizing with chemically active CO_2, the shift of the isotropic temperature of {CO_2/PEO_{114}-*b*-PMA(Az)$_{20}$} system shows a linear relationship at low pressures, up to 8 MPa, in this range of pressure the isotropic transition temperature decreases with an increase of *p*, which is the opposite tendency to that under Hg pressure. T_{iso} approaches to a constant value at higher pressures, up to 50 MPa, as shown with the investigation of {CO_2/PEO_{114}-*b*-PMA(Az)$_{40}$} system on Fig. 5. Extrapolations of the relationships of T_{iso} *vs*. pressure of both Hg and CO_2 to atmospheric pressure showed a good agreement and gave 385.0 K, in accordance with DSC results. The activity of compressed CO_2 above its critical temperature is likely to be changed continuously by changing the pressure from GCO_2 (5 MPa) to $SCCO_2$ (8 MPa). In the latter case of relatively low CO_2 pressure, pressure facilitates the sorption of the fluid into the polymer and then the polymer chains gain degrees of movement. The gas in the supercritical state acts as 'lubricant' between the polymer chains (i.e. plasticization effect) [15] which have higher ability to orient, yielding the decrease of T_{iso}; in this scheme, the PEO part is dissolved in $SCCO_2$ and the interface, i.e. junction point, between chain end of PEO and methacrylate PMA(Az) acquires molecular mobility. At higher $SCCO_2$ pressures the hydrostatic effect overcomes the plasticization effect. The T_{iso} behaviour reflects the sorption of gas into the polymer with the concomitant volume change, that is to say, the increase of solubility and swelling occurring first at low pressure and then plasticization levels off; the restriction of molecular motion appears at high pressure, thus T_{iso} should tend to a limit. The liquid crystalline state might be influenced by the purity of the sample and since the PMA(Az) part is the site where a large sorption of CO_2 takes place, then the liquid crystalline state could disappear. In our study, T_{iso} being directly related to the amount of CO_2 absorbed, CO_2 sorption should be small and not disturb the molecular interactions as well as the intermolecular distance.

The temperature range of the isotropic phase change becomes narrower with increasing pressure. This can be shown quantitatively by calculating the corresponding entropy ΔS_{iso} of the system from the

Table 1 Increase of diameters of PEO cylinders and of distances between PEO cylinders under $SCCO_2$

	Un-modified	$SCCO_2$ (313 K, 9 MPa)		$SCCO_2$ (351 K, 9 MPa)	
		Just after treatment	2 weeks after at (298 K, 0.1 MPa)	Just after treatment	2 weeks after at (298 K,0.1 MPa)
Diameters of PEO cylinders/nm	11.8±0.2	13.6±0.5	11.9±0.4	18.4±1.3	12.0±0.6
Distances between PEO cylinders/nm	19.8±0.4	21.2±0.6	21.2±0.6	24.9±1.6	21.4±0.8

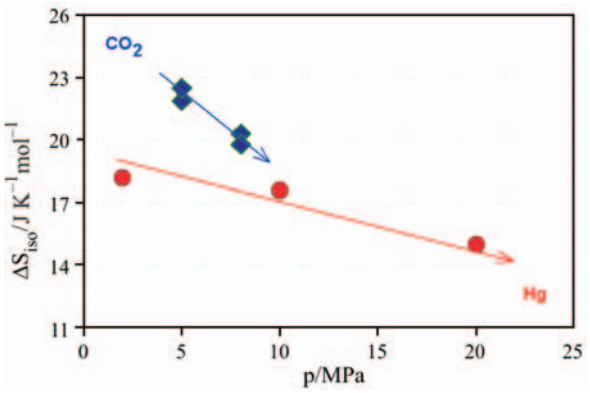

Fig. 6 Isotropic entropy ΔS_{iso} as a function of pressure for {PEO_{114}-*b*-$PMA(Az)_{20}$} system under Hg (closed circles) and CO_2 (runs 2nd and 3rd, closed diamonds) pressures. The values are given per unit *n* of degree of $PMA(Az)_n$ polymerization

thermal effect. Figure 6 represents ΔS_{iso} for PEO_{114}-*b*-$PMA(Az)_{20}$ under Hg and CO_2 respectively. The results clearly demonstrate the lowering of the isotropic entropy in the presence of dissolved CO_2 at pressure below 12 MPa. The slope $d\Delta S_{iso}/dp$ gives –0.18 with Hg and –0.72 with CO_2 that shows the strong dependence of ΔS_{iso} with CO_2. T_{iso} and ΔS_{iso} seem to vary linearly according to the Clapeyron equation in the range of pressures investigated. Accurate determination of the pressure dependence of CO_2 in gaseous and supercritical states is very important because it permits to control the 'easiness' of molecular interactions: {CO_2/polymer} interactions are higher than {Hg/polymer} interactions. In {Hg/PEO_{114}-*b*-$PMA(Az)_{20}$} system, polymer/liquid crystal interactions are favoured by the hydrostatic pressure effect whereas in {CO_2/PEO_{114}-*b*-$PMA(Az)_{20}$} system gas/polymer interactions are predominantly favoured in presence of $SCCO_2$. The hydrostatic effect by Hg influences the 'physical interactions' between PEO polymer and PMA(Az) liquid crystal moieties; while when the pressure is exerted by CO_2 the gas not only imposes a hydrostatic effect but also acts as an active solvent which penetrates the molecular organization, i.e. penetrates into the block copolymer, and preferably interacts with the PEO polymer part. In this process, the dissolved gas reduces the intermolecular interactions, and induces more degree of freedom. The high depression of ΔS_{iso} at 8 MPa is the result of two contributions: entropy of azobenzene at the isotropic transition and mixing entropy ΔS_{mixing} of azobenzene (and of polymer) with CO_2. Then, CO_2 in the gas state (GCO_2) appears as a 'poor' solvent at 5 MPa whereas in the supercritical state ($SCCO_2$) at 8 MPa becomes a more efficient solvent and ΔS_{mixing} becomes smaller. This indicates that the extent of entropy loss depends strongly on the pressure medium.

The effect of supercritical CO_2 on the nano-scale ordered structure of PEO_m-*b*-$PMA(Az)_n$ di-block copolymers was investigated by means of atomic force microscopy AFM, especially to compare the behaviour of both hydrophilic and hydrophobic domains under CO_2 pressure (Figs 7, 8). The di-block copolymer PEO_{114}-*b*-$PMA(Az)_{46}$ was investigated under the form of a film laid on a polyethylene terephthalate (PET) support. PEO domains correspond to the darker areas (accentuated with circles). The image on the left hand side represents the unmodified structure, while on the right hand side two modified structures after 1 hour exposure under 9 MPa of CO_2 at 313 K (upper) and 351 K (lower), respectively, are shown Under the $SCCO_2$ treatment, the PEO cylinders kept the hexagonal structure with an increase in diameter of the nano-tubes. The diameter of PEO cylinders varied from 11.8 nm for the un-modified sample to 13.6 and 18.4 nm for the modified samples at 313 and 351 K, respectively (Table 1). In addition, the distance between the PEO cylinders slightly increased after treatment. Expansion of the PEO cylinders was due to the absorption of $SCCO_2$ [16] with increasing temperatures. As the PMA(Az) domain surrounding the PEO cylinders was in the smectic C (SmC) phase, PEO cylinders could expand by dissolving $SCCO_2$ at 351 K. Figure 8 shows a schematic representation of the SmC phase of PMA(Az) domains surrounding the PEO cylinders with the sorption of $SCCO_2$ into PEO cylinders. The nano-PEO_m structure, i.e. diameter of PEO cylinders, returned to the initial state at room temperature T_{room} (298 K, 0.1 MPa) after two weeks. The $PMA(Az)_n$ domains at T_{room} were considered as a supercooled SmC phase due to the following reasons. The melting enthalpy of $PMA(Az)_n$ in PEO_{114}-*b*-$PMA(Az)_{20}$ (2.2 J g^{-1} of repeating PMA(Az) unit) was smaller than the melting enthalpy of homo -$PMA(Az)_{60}$ (6.4 J g^{-1} of repeating PMA(Az) unit), observed by DSC under N_2 at 0.1 MPa. Most of $PMA(Az)_n$ in PEO_m-*b*-$PMA(Az)_n$ remained in the amorphous state. After CO_2 modification the temperature was decreased to room temperature under 9 MPa, that means $SCCO_2$ changed to liquid state, and then the pressure was suddenly decreased and CO_2 evaporated. The volume occupied by CO_2 remained as free volume. This surplus of free volume disturbed the crystallization of both PEO and PMA(Az) domains; in that sense we consider that the supercooled state remained. After modification by $SCCO_2$, the liquid crystal PMA(Az) matrix being in the supercooled SmC phase and the molecular mobility remained at room temperature; the PEO part being in the liquid state, the molecules, favoured by gas diffusion phenomena, could move easily and return to the thermodynamic equilibrium inducing thus liquid

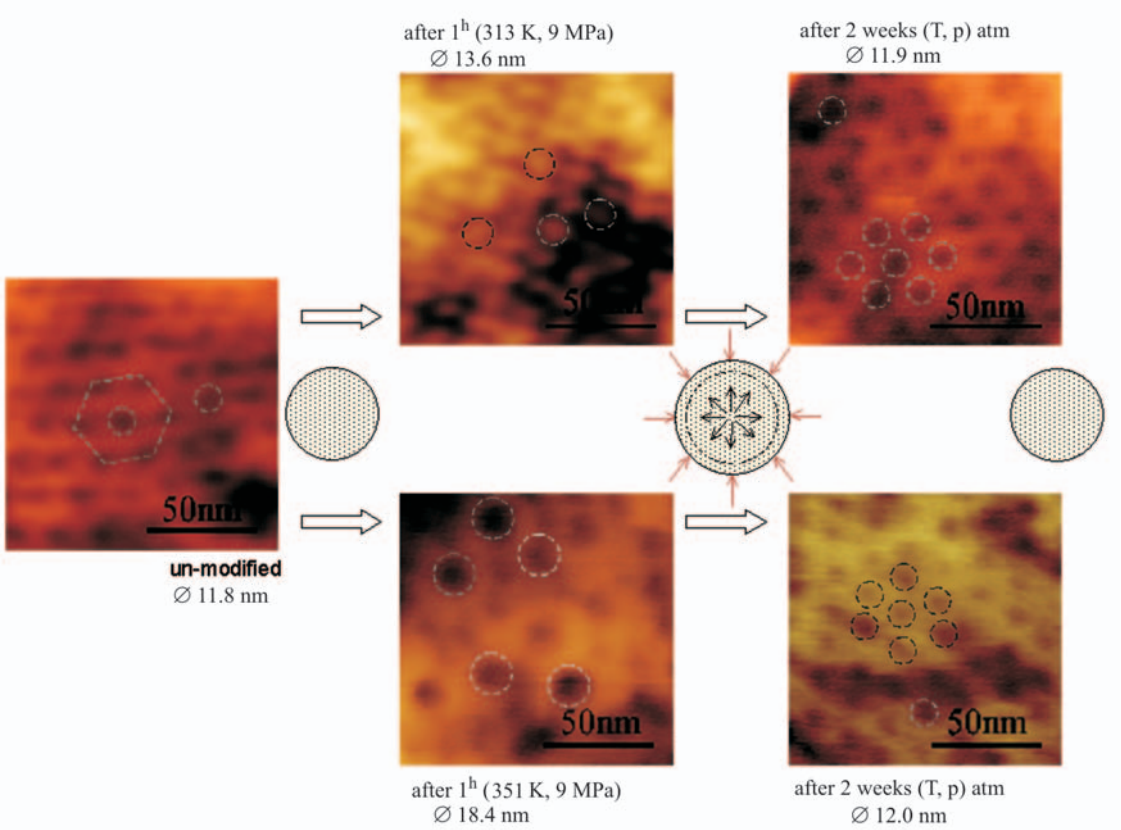

Fig. 7 Effect of $SCCO_2$ and of the temperature on the fine nano-scale ordered structure with hexagonal-packed PEO cylinders in $\{CO_2/PEO_{114}$-*b*-$PMA(Az)_{46}\}$ system at 9 MPa, illustrated with AFM topological images. PEO domains correspond to the darker areas (accentuated with circles). The schematic picture illustrates the expansion changes of PEO cylinders

crystal copolymers interactions. As a consequence, the swollen irregular nano-structure could return to the highly ordered nano-structure after a few weeks at room temperature. These results confirm the ability of $SCCO_2$ to modify the copolymer interfacial self-organization through more efficient hydrophilic $\{SCCO_2/PEO_m\}$ interactions (Fig. 7).

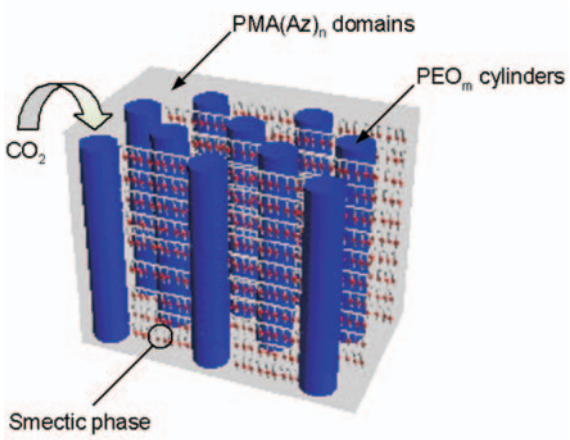

Fig. 8 Schematic illustration showing the liquid crystal PMA(Az) domains surrounding the PEO cylinders in the SmC phase; PEO cylinders can expand under $SCCO_2$ sorption

Conclusions

A first approach to ascertain the interactions of CO_2 with amphiphilic di-block copolymers was reported with the thermophysical properties of the isotropic transition. The chemical stress results essentially from the sorption of the supercritical fluid. The interactions with the hydrophilic part PEO in $\{SCCO_2/PEO_m\}$ were more favoured than the interactions with hydrophobic PMA(Az) domains in $\{SCCO_2/PMA(Az)_n\}$. A comparison of the effects induced under either CO_2 or Hg hydrostatic pressures suggested that the gas-polymer interactions (i.e. gas solubility) were responsible for the shift to lower values of T_{iso} and ΔS_{iso} at least at relatively low pressures up to 10 MPa.

Acknowledgements

This work is a contribution to 'The Creation and Transcription of Reliable Macromolecular Templates based on Phase-separated Nano-structures Project' (Research Director: Dr. Tomokazu Iyoda). The financial support of the Core Research for Evolutional Science and Technology (CREST) Program,

which is one of the special programs of Japan Science and Technology (JST), is gratefully acknowledged.

References

1 B. Flaconnèche, J. Martin and M. H. Klopffer, Oil and Gas Sci. and Technology – Rev. IFP, 56 (2001) 245.
2 S. A. E. Boyer and J-P. E. Grolier, Polymer, 46 (2005) 3737.
3 J. B. McClain, D. E. Betts, D. A. Canelas, E. T. Samulski, J. M. DeSimone, J. D. Londono, H. D. Cochran, G. D. Wignall, D. Chillura-Martino and R. Triolo, Science, 274 (1996) 2049.
4 H. Yoshida, K. Watanabe, R. Watanabe and T. Iyoda, Trans. Materials Res. Soc. Jpn., 29 (2004) 861.
5 Cagniard de la Tour, C. Ann. Chim., 22 (1822) 410.
6 C. L. Phelps, N. G. Smart and C. M. Wai, J. Chem. Educ., 73 (1996) 1163.
7 A. Seeger, D. Freitag, F. Freidel and G. Luft, Thermochim. Acta, 424 (2004) 175.
8 Z. Zhang and Y. P. Handa, Macromolecules, 30 (1997) 8505.
9 K. Watanabe, Y. Tian, H. Yoshida, S. Asaoka and T. Iyoda, Trans. Materials Res. Soc. Jpn., 28 (2003) 553. Y. Tian, K. Watanabe, X. Kong and T. Iyoda, Macromolecules, 35 (2002) 3739.
10 S. L. Randzio, J-P. Grolier, J. Zaslona and J. R. Quint, French patent 9109227, Polish patent 295285 – S. L. Randzio and J-P. E. Grolier, Anal. Chem., 70 (1998) 2327.
11 S. A. E. Boyer, S. L. Randzio and J-P. E. Grolier, J. Polym. Sci., 44 (2006) 185.
12 K. Kamata, R. Watanabe, S. Shoda, D. Aoki, K. Watanabe, K. Ogawa, H. Tokimori, M. Komura, A. V. S. Sainath and T. Iyoda, Polym. Prepr. Japan, 54 (2005) 5437.
13 S. A. E. Boyer, J-P. E. Grolier, H. Yoshida and T. Iyoda, Polym. Prepr. Japan, 1, 54 (2005) 815. S. A. E. Boyer, L. Pison, C. Iwamoto, J-P. E. Grolier, H. Yoshida and T. Iyoda, Polym. Prepr. Japan, 2, 54 (2005) 3215.
14 H. Yoshida, T. Yamada, R. Watanabe, K. Watanabe, T. Iyoda, T. Delrieu and J-P. E. Grolier, IUPAC World Polymer Congress Macro (2004) Proceedings, 2.3.3. S. A. E. Boyer, J-P. E. Grolier, H. Yoshida and T. Iyoda, J. Polym. Sci., (2006) submitted.
15 A. F. Ismail and W. Lorna, Sep. Pur. Technol., 27 (2002) 173.
16 H. Lin and B. D. Freeman, J. Membr. Sci., 239 (2004) 105.

DOI: 10.1007/s10973-006-7633-z